U.S. DEPARTMENT OF ENERGY | Office of Science

DOE/SC-CM-25-002

FY 2025 Second Quarter Performance Metric: Demonstrating Modeling of Urban Hydrology and Flooding Using the E3SM Land-River Model with a New Urban Hydrology Module

L Ruby Leung
Gautam Bisht
Seife Eriget
Hongyi Li
Lingcheng Li

April 2025

DISCLAIMER

Contents

1.0 Product Definition 1
2.0 Product Documentation 2
2.1 A New Representation of Urban Hydrology: MOSART-urban 2
2.2 Runoff Forcing From a Calibrated ELM Simulation 5
2.3 MOSART-urban Simulations Driven by the ELM Runoff Over CONUS 6
3.0 Results 7
3.1 Evaluation of MOSART-urban in the Houston Metropolitan Area 7
3.2 Results From ELM Calibration 10
3.3 CONUS-wide MOSART-urban Simulations Driven by the ELM Runoff 11
4.0 Summary and Future Work 13
5.0 References 14

Figures

Figure 1. Conceptual diagram of the MOSART-urban framework. 3
Figure 2. Diagram of a storm-sewershed: (a) a plan view of major elements and their flow exchanges; (b) a cross-section view of urban impervious surface, street inlets, stormwater pipes, and their connections. 4
Figure 3. Selected watersheds in Houston, TX, with their USGS station identifiers. 5
Figure 4. CONUS domain of the ELM-MOSART-urban simulations. Each dot represents an urban watershed with an urban fraction no less than 30% of its area, which is indicated by the dot size. 6
Figure 5. Annual maximum floods (AMFs) in 2003-2020, shown as the ranked AMF value, from the observed streamflow (Q_{obs}) and simulations by MOSART-urban (Q_{sim}) and NWM (Q_{sim}(NWM)). The numbers in the parentheses are the imperviousness levels to indicate the degree of urbanization in each watershed. 7
Figure 6. Mean monthly streamflow in 2016-2020 from the observed streamflow (Q_{obs}) and simulations by MOSART-urban (Q_{sim}) and NWM (Q_{sim}(NWM)). The numbers in the parentheses are the imperviousness levels. 8
Figure 7. Impact of BUSNs on hourly hydrographs during Hurricane Harvey as estimated by comparing simulations with and without BUSNs. 9
Figure 8. The interplay between hourly rainfall, impervious zone overflow, and BUSN outflow during Hurricane Harvey at three watersheds with high imperviousness. The total streamflow (Q_{sim}) is the sum of the impervious overflow and BUSN overflow. 10
Figure 9. Evaluation of ELM-simulated water table depth (WTD) and standing surface water dynamics. (a) Benchmark WTD dataset of Fan et al. (2013) and ELM-simulated WTD with (b) default f_{drain} and (c) calibrated f_{drain}. (d) Benchmark inundated surface water fraction, f_{ssw}, dataset and ELM-simulated f_{ssw} with (e) default f_c and (f) calibrated f_c. 11
Figure 10. KGE at the selected USGS stations with significant urban developments in their drainage areas. 11
Figure 11. Change of the KGE values between simulations with and without BUSNs. 12

Figure 12. Scatter plots of KGE, R2, and NRMSE between MOSART-urban simulations with and without BUSNs. Higher KGE and lower NRMSE values for the simulation with BUSN than without BUSN indicate improvements in simulating the magnitude of daily streamflow when BUSNs are included in the model. 13

Figure 13. Comparison of annual maximum daily flood peaks, shown as the AMF for different return periods, at four representative stations simulated by MOSART-urban with and without BUSNs. The areal urban fractions of the four stations are shown by the numbers inside the parenthesis above each panel. 13

1.0 Product Definition

Rapid global urbanization has fundamentally modified hydrologic processes by altering hydrologic conditions (e.g., imperviousness, soil compaction) and intensifying extreme weather events. Combined with the evolving environments, the impact of urbanization may be amplified (Grimm et al. 2008). These changes significantly impact urban hydrologic cycles and often lead to increased storm runoff and flood risks. Below-ground urban stormwater networks (BUSNs) are essential for mitigating urban floods, underscoring why their modification—primarily through upgrades or duplication, such as replacing pipes with larger ones—remains a predominant, albeit costly and disruptive, flood mitigation strategy (Burns et al. 2015; Chocat et al. 2021; Argue and Pezzaniti 2012). Using observations, previous studies have provided evidence of the hydrologic impacts of urbanization at the regional scale and decadal and longer timescales (Yang et al. 2013; Miller and Hutchins 2017). Through numerical experiments, Earth system models (ESMs) are important tools to further our understanding of the various pathways of how urbanization impacts hydrologic processes and its potential to exacerbate or mitigate flooding in an evolving environment with increasing extreme precipitation. However, current ESMs lack the spatial resolutions needed to resolve fine-scale heterogeneity in urban environments (e.g., completely missing BUSNs and their interactions with urban surface hydrologic processes). This oversimplification leads to inaccuracies in predicting urban floods and other urban hydrologic processes such as infiltration, evapotranspiration, and groundwater recharge.

Hydraulics-based models are invaluable for detailed urban hydraulic and hydrologic simulations. The integration of storm sewer networks into hydrologic-hydraulic models is essential for accurately representing urban flood dynamics, as these networks play a pivotal role in managing stormwater runoff and mitigating flood risks (Guo et al. 2021). In these models, BUSNs are represented at the level of individual stormwater pipes, with water and other fluxes simulated using hydraulic equations. Because of the intensive data requirements, expensive computational costs, and site-specific parameters not being easily transferable, hydraulics-based models are impractical for use in representing urban hydrology in ESMs.

Recently, a new modeling strategy was developed to represent BUSNs directly at the network level, capturing their main hydrologic functions instead of modeling individual pipes and their interactions. This strategy features a BUSN parameterization based on Graph Theory to delineate storm-sewersheds within a watershed, derive sub-BUSNs associated with each storm-sewershed, and determine the BUSN-relevant parameters a priori (Chegini and Li 2022). This modeling strategy has been implemented as a new urban module that is physically based, parameter-parsimonious, and computationally efficient within the Model for Scale Adaptive River Transport (MOSART-urban) (Chegini et al. in press), holding promises to be applied at large spatial and long temporal scales without losing sight of below-ground urban hydrologic processes.

In this report, we first demonstrate the MOSART-urban modeling framework in nine representative watersheds exhibiting various levels of urbanization, ranging from natural to highly developed watersheds in the Houston metropolitan area. As a first step to integrate MOSART-urban into the Energy Exascale Earth System Model (E3SM), we further demonstrate the performance of MOSART-urban driven by the runoff simulated by the calibrated E3SM Land Model (ELM) in simulations across river basins in the contiguous United States (CONUS). Validation against observed daily streamflow shows that MOSART-

urban can capture small-to-large flood peaks and seasonal and annual water balance over the nine watersheds in the Houston area, with better performance compared to the National Water Model. MOSART-urban simulations driven by the runoff simulated by ELM show good performance in ~65% of the 299 watersheds across CONUS, with an urban fraction > 30%. Comparisons of MOSART-urban with and without BUSNs for both the simulations over the Houston metropolitan area, a region chosen for its diverse landscapes and a rich history of floods, and across CONUS demonstrate the flood-mitigation capacity of BUSN, which increases with the urban area coverage in the watersheds. MOSART-urban bridges the gap between detailed hydraulic and large-scale hydrologic models, providing a valuable tool for urban flood prediction and management across broader spatial and temporal scales and for Earth system modeling of the impacts of urbanization on the regional and global water cycles.

2.0 Product Documentation

This report documents the MOSART-urban modeling framework for representing network-level storm drainage pipes and urban hydrologic processes. MOSART-urban was first validated in the Houston metropolitan area. To test MOSART-urban within E3SM, ELM was calibrated using observed groundwater table depth and inundated surface water fraction data to constrain the simulation. The ELM ELM-simulated runoff was then used to drive MOSART-urban simulations with and without BUSNs to isolate their impacts on streamflow and flood peaks in CONUS river basins with at least 30% urban coverage.

2.1 A New Representation of Urban Hydrology: MOSART-urban

MOSART-urban is documented by Chegini et al. (in press), along with the development of an algorithm for deriving the topology of BUSNs described in Chegini and Li (2022). Here, we introduce the conceptualization of the modeling framework while details of the governing equations, parameter calibration, and data preparation are provided by the aforementioned two references.

In MOSART, a natural watershed can be conceptualized into three hydrologically connected components with distinct hydrologic functions (Li et al. 2013): 1) hillslopes, where the natural landscape and soil conditions control runoff generation and routing processes, 2) a sub-network channel, which receives runoff from hillslopes and discharges the runoff into a single main channel, and 3) the main channel, which receives the discharge from sub-network and connects the local watershed with its upstream and/or downstream watersheds. For urban watersheds, this conceptualization is extended by adding a fourth component, storm-sewersheds, where urban runoff generation and routing processes are governed by man-made infrastructure such as BUSNs and impervious areas, as shown in Figure 1. We define a storm-sewershed as an urban area (typically a mixture of both pervious and impervious surfaces) and its corresponding BUSN that contributes stormwater to rivers and other surface waterbodies via a single outfall. Such a network-level representation of stormwater pipes avoids detailed hydraulic modeling of individual pipes and their interactions. Yet it captures the major hydrologic functions of BUSNs at the watershed scale, including 1) interception capacity, i.e., the maximum amount of surface runoff from impervious areas that can be captured and passed into stormwater pipes via street inlets and catch basins (Chegini and Li 2022); 2) conveyance capacity, i.e., the maximum discharge that can be routed through BUSN pipes into receiving water bodies via outfalls; and 3) transient storage capacity, i.e., the total amount of water that can be stored in all the BUSN pipes during a storm event.

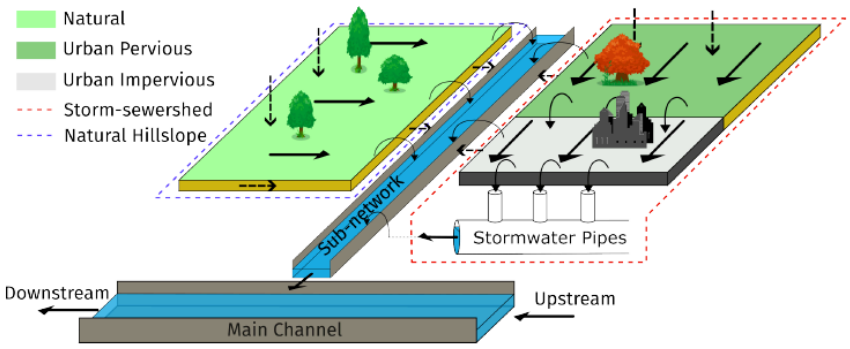

Figure 1. Conceptual diagram of the MOSART-urban framework.

BUSNs are designed to rapidly direct stormwater to the nearest waterbodies, minimizing potential flooding impacts (Brown et al. 2009). Considering that outfalls are the only locations where a BUSN discharges stormwater back to surface water and that these outfalls are distributed over urban areas, we define a storm-sewershed based on a sub-BUSN. Within a storm-sewershed, stormwater pipes are well-connected, and all contribute to a single outfall that discharges into a surface waterbody, but they are not connected to the other sub-BUSNs even in the same watershed. We can thus represent the urban portion of a watershed into several storm-sewersheds using the techniques described in Chegini and Li (2022) based on Graph Theory.

As shown in Figure 2, a storm-sewershed consists of both surface and subsurface elements that collectively determine the urban hydrologic responses to storms, including urban pervious surfaces (e.g., lawns, parks), impervious surfaces (such as streets, buildings, and parking lots), a sub-BUSN, an outfall connecting the sub-BUSN to the sub-network channel (or the main channel if there is no sub-network channel), and soils surrounding the stormwater pipes within the sub-BUSN. For simplicity, we lump all urban pervious surfaces into a single pervious surface zone. Similarly, we define a lumped impervious surface zone. Considering that most streets can store some surface runoff temporarily before discharging into the sub-BUSN via inlets, we also assume there is a limited storage capacity in the urban impervious surface zone. Within each sub-BUSN, there are several stormwater pipes. We denote the pipe directly connected to the outfall as the main pipe and the rest as the tributary pipes. These tributary pipes function as the connection between street inlets and the main pipe. Thus, we replace all tributary pipes that connect an inlet to the main pipe with a single equivalent pipe. As a result, in our simplified sub-BUSN, there is a one-to-one match between a street inlet and a tributary pipe, i.e., the number of tributary pipes is the same as the number of street inlets.

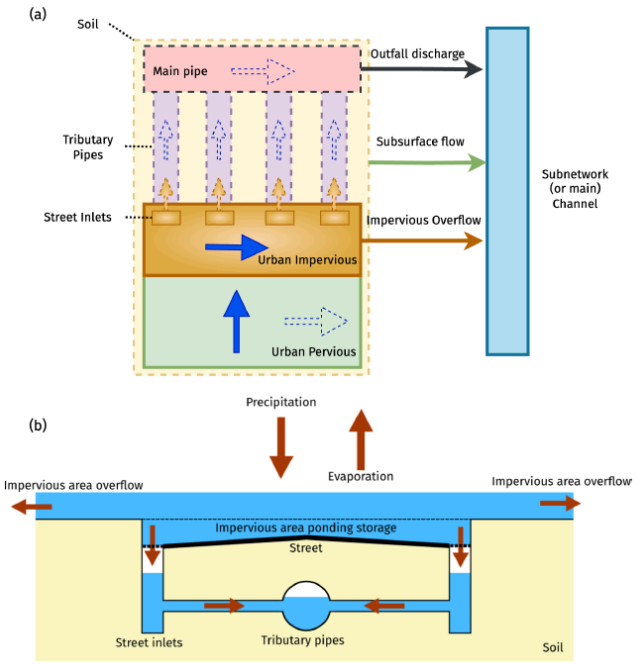

Figure 2. Diagram of a storm-sewershed: (a) a plan view of major elements and their flow exchanges; (b) a cross-section view of urban impervious surface, street inlets, stormwater pipes, and their connections.

Overall, when rain falls on an urban watershed, any surface runoff generated from the urban pervious surface zone will be routed into the impervious surface zone and join the surface runoff generated there. The ponding water on the impervious surface zone may evaporate into the atmosphere, enter into the sub-BUSN zone via street inlets distributed along streets, or overflow across the surface zones into the sub-network or main channel when the amount of water stored in the impervious surface zone exceeds its storage capacity (i.e., urban flooding occurs). Tributary pipes receive stormwater via street inlets and discharge to the main pipe. The main pipe discharges into the sub-network channel via the outfall. Note that there are two major types of urban sewer systems: separate sewer systems, where two separate pipe systems carry stormwater and sanitary sewage, respectively, and combined sewer systems, where a single pipe system exists for conveying both stormwater and municipal sewage. The current implementation only deals with stormwater, leaving out sanitary sewage for future work.

MOSART-urban represents major hydrologic processes, including hillslope processes (runoff generation and routing across natural areas), storm-sewershed processes (runoff generation and routing across urban areas), and routing through the sub-network and main channels. The detailed governing equations used to represent these processes are described in Chegini et al. (2025). A four-stage third-order Strong Stability Preserving Runge-Kutta time marching scheme is used to solve all the governing equations (Durran 2010). Methods used to determine the model parameter values and prepare the hydrography data are described in detail in Chegini et al. (2025).

To validate MOSART-urban, a simulation was performed over nine watersheds in Houston, Texas (Figure 3) for 2003-2020 based on the availability of daily observed streamflow data from the United States Geological Survey (USGS) stations at the watershed outlets. As a region with diverse landscapes and a rich history of floods, this demonstration allows us to evaluate the model's performance across a spectrum of urban environments and underscore the model's adaptability and promises for broader

applications. Observations for 2003-2015 were used for model calibration, and data for 2016-2020 were used for model validation. The North American Land Data Assimilation System Phase 2 (NLDAS2) (Xia et al. 2012) at 0.125° x 0.125° grid resolution was used to provide atmospheric forcing by remapping from the grids to the watersheds. The retrospective hourly results from the National Water Model (NWM) version 3 (Cosgrove et al. 2024) for 1979-2023 were also included for comparison. NWM is a continental-scale hydrologic model developed by the U.S. National Oceanic and Atmospheric Administration (NOAA) for forecasting streamflow and inundation over the U.S. NWM has 14 calibrated parameters and does not include BUSNs.

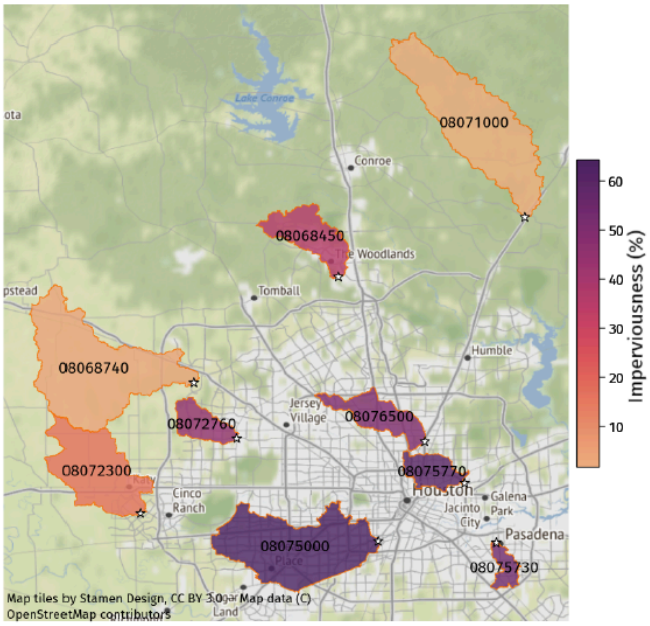

Figure 3. Selected watersheds in Houston, TX, with their USGS station identifiers.

2.2 Runoff Forcing From a Calibrated ELM Simulation

To test the coupling between ELM and MOSART-urban, an ELM simulation was performed to provide the runoff forcing for MOSART-urban. The runoff forcing was generated using a modified ELM version 2 (Golaz et al., 2022) with improved treatment of subgrid topographic effects on solar radiation (Hao et al., 2021) and pluvial inundation dynamics (Xu et al., 2024). ELM simulations were performed for 2000–2019 over CONUS at 1 km grid spacing and driven by the atmospheric forcing from NLDAS2. The recently developed 1 km global surface parameter dataset of Li et al. (2024) was used to generate the ELM surface dataset. The ELM simulations were performed in the satellite phenology mode that used leaf and stem area index corresponding to the year 2010. A two-stage ELM model calibration was used to improve the simulation of water table depth, WTD, and inundated surface water fraction, f_{ssw}, against benchmark datasets. First, using the approach of Bisht et al. (2018), a set of six 40-year-long simulations was performed with different values for the highly uncertain subsurface drainage parameter, f_{drain}. A nonlinear relationship was fitted between f_{drian} and the simulated WTD for each grid, which was used to estimate an optimal f_{drain} value based on the benchmark WTD dataset of Fan et al. (2013). Next, following the approach of Xu et al. (2024), an additional set of five ELM simulations was performed to calibrate a pluvial flood dynamics parameter, f_c, to improve the simulation of f_{ssw} against the Global Land Analysis & Discovery dataset (Pickens et al., 2020).

2.3 MOSART-urban Simulations Driven by the ELM Runoff Over CONUS

To use the ELM-simulated runoff as forcing to MOSART-urban, a mapping was performed between the ELM 1 km grids and the HUC12 watersheds, since HUC12 watersheds are used as the computational units of MOSART-urban. Using the HUC12 watershed boundary shapefile over CONUS, a raster at the same 1 km mesh as the ELM simulations was created. For each HUC12 watershed, the ELM-simulated surface and subsurface runoff at individual grid cells were used to calculate the HUC12 mean runoff separately for urban and non-urban areas based on the land use and land cover data from the ELM surface parameters. The aggregated urban and non-urban runoffs were then processed into specific input formats required by MOSART-urban, which explicitly accounts for impervious surface effects in urban areas. For the CONUS simulations, MOSART-urban was configured to simulate only the routing processes in both the natural channel network and BUSNs, providing a more realistic representation of urban hydrology within the HUC12 watersheds across CONUS.

To evaluate the hydrologic impacts of urban stormwater infrastructure, we conducted paired simulations using the ELM runoff to drive the MOSART-urban routing scheme with and without BUSNs. The BUSN-enabled simulation incorporates urban drainage infrastructure, altering both peak and low flows. Model performance was assessed using multiple statistical metrics, including the Kling-Gupta Efficiency (KGE), Normalized Root Mean Square Error (NRMSE), and R^2 (square of the correlation coefficient), by comparing the daily streamflow from both simulations against observations from selected urban USGS stations. Additionally, inter-simulation comparisons were conducted to quantify the net effects of BUSNs on streamflow variability and flood peak mitigation. Figure 4 highlights the spatial distribution of urbanized basins, defined as basins with >30% urban coverage, analyzed in this study. Larger basins generally have smaller urban fractions, and more urbanized basins are located in the eastern U.S.

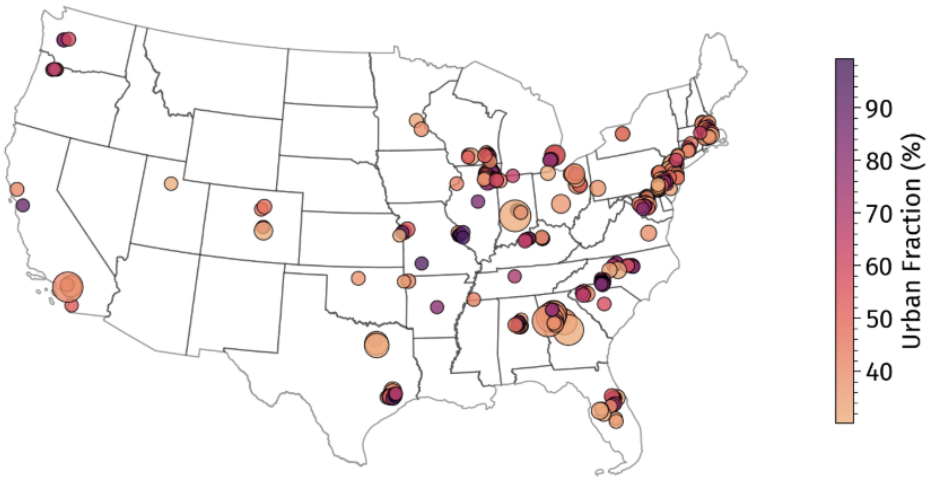

Figure 4. CONUS domain of the ELM-MOSART-urban simulations. Each dot represents an urban watershed with an urban fraction no less than 30% of its area, which is indicated by the dot size.

3.0 Results

3.1 Evaluation of MOSART-urban in the Houston Metropolitan Area

To evaluate the MOSART-urban simulation over nine watersheds in the Houston area (Figure 3), we compare the observed and MOSART-urban and NWM simulated annual maximum daily floods (AMFs) from 2003 to 2020. Figure 5 shows that MOSART-urban can well capture flood peaks across various magnitudes. Compared to NWM, MOSART-urban has much smaller biases in simulating AMFs at eight of the nine watersheds. Furthermore, comparing the mean monthly streamflow, Figure 6 shows similar performance between MOSART-urban and NWM in capturing seasonal water balance at the natural watersheds (08068740 and 08071000), but MOSART-urban performs much better at all urban watersheds. Despite the much higher performance compared to NWM, there are still noticeable biases in MOSART-urban simulations of flood peaks. These biases can be attributed to (1) biases in the precipitation forcing data, particularly during extreme rainfall events like Hurricane Harvey (Chen et al. 2020), and (2) the runoff scheme used in MOSART-urban, which centers on saturation excess runoff that occurs when the soil becomes fully saturated and cannot absorb additional water. This runoff scheme tends to underestimate flood peaks by neglecting infiltration excess runoff, which happens when rainfall intensity exceeds the soil's infiltration capacity and is particularly relevant during high-intensity precipitation events like Hurricane Harvey. However, these MOSART-urban biases are notably less than those in NWM. The significant underestimation of AMFs (Figure 5) and yet the overestimation of mean monthly streamflow (Figure 6) by NWM indicates that MOSART-urban outperforms NWM in simulating both the flood peaks and seasonal water balance. The superior performance of MOSART-urban, despite using only seven parameters compared to the NWM's 14, demonstrates the effectiveness and efficiency of the MOSART-urban parameterization strategy for urban areas.

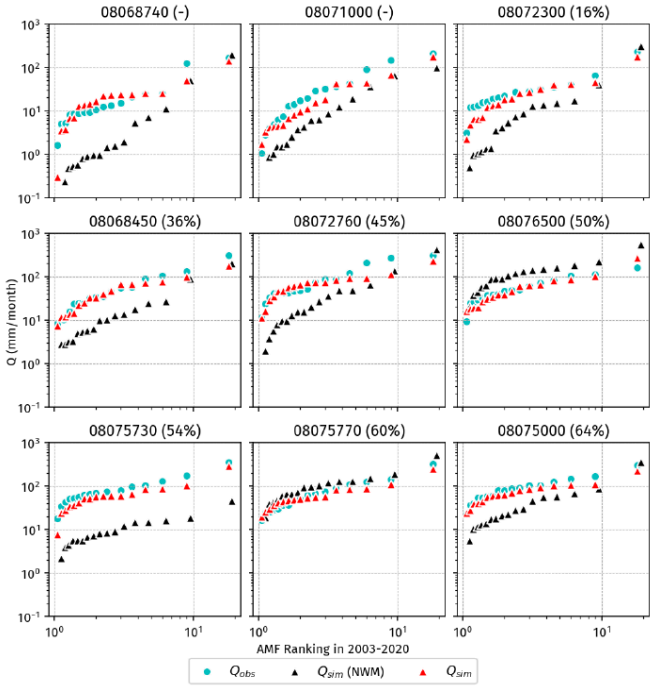

Figure 5. Annual maximum floods (AMFs) in 2003-2020, shown as the ranked AMF value, from the observed streamflow (Q_{obs}) and simulations by MOSART-urban (Q_{sim}) and NWM (Q_{sim}(NWM)). The numbers in the parentheses are the imperviousness levels to indicate the degree of urbanization in each watershed.

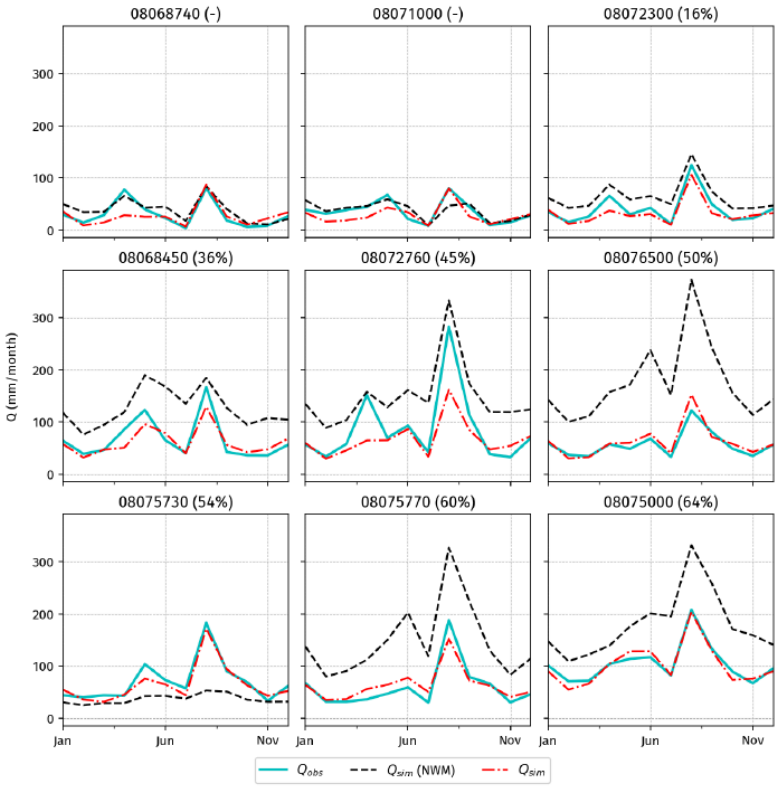

Figure 6. Mean monthly streamflow in 2016-2020 from the observed streamflow (Q_{obs}) and simulations by MOSART-urban (Q_{sim}) and NWM (Q_{sim}(NWM)). The numbers in the parentheses are the imperviousness levels.

To examine whether MOSART-urban is getting the right answer for the right reasons and gain deeper insights into the impacts of BUSNs on urban flood reduction, we examine the Hurricane Harvey event across nine watersheds. The flood event caused by Hurricane Harvey lasted from August 27 to 29, 2017. Simulations were performed with and without BUSNs to quantify the net effects of BUSNs. As expected, there is no noticeable difference between the two simulations in watersheds that are natural or have small imperviousness (Figure 7). However, in other watersheds, BUSNs noticeably reduce the magnitude of flood peaks, but the peak timing is not significantly delayed. For multi-day flood events like Hurricane Harvey, the flood reduction effect is stronger for the first flooding day (August 27th) than for the later days. This is because the designed BUSN capacities for interception and transient storage of excess stormwater are largely reached during the first day, leaving little capacity for subsequent days. Therefore, the flood reduction effect is weakened in the later stage of multi-day flood events. This phenomenon is more pronounced for watersheds (e.g., 08075730, 08075770, 08075000) with high imperviousness.

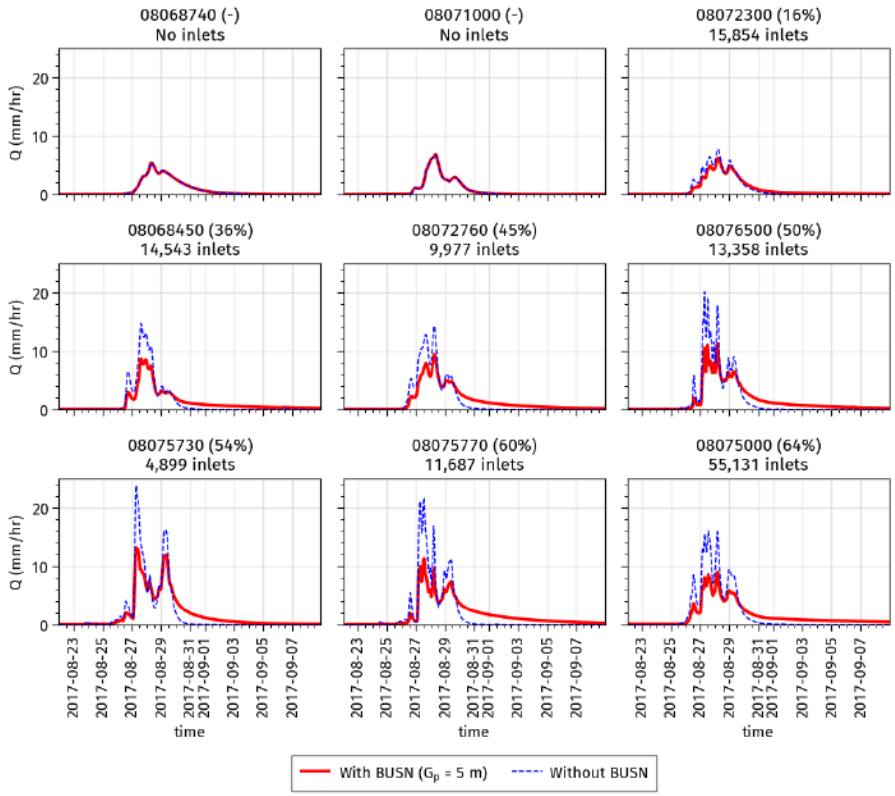

Figure 7. Impact of BUSNs on hourly hydrographs during Hurricane Harvey as estimated by comparing simulations with and without BUSNs.

The flood reduction effects observed in Figure 7 can be better understood by examining the underlying processes. Figure 8 depicts the major processes driving streamflow variability in watersheds 08075730, 08075770, and 08075000 during Hurricane Harvey: rainfall variability, overflow from the impervious zone, and BUSN outflow. Impervious zone overflow responds more directly to rainfall variations and exhibits much higher temporal variability than BUSN outflow. The high temporal variability in impervious zone overflow only partially propagates to that of streamflow, due to the dispersion effects of the channel routing processes in the sub-network and main channels. BUSN outflow exhibits a more dispersed pattern, mainly due to the routing process through the BUSN pipes with very mild slopes. BUSN essentially offers substantial buffering of stormwater, which eventually helps reduce flood peaks. This is consistent with the fact that one of the major purposes of BUSNs is the safe, gradual conveyance of stormwater toward the receiving rivers. Additionally, we can discern from Figure 8 that the impervious overflow contributes the most on the first two days with the highest precipitation (August 27th and 28th), whereas the BUSN outflow contributes the most to the streamflow on the last day of the rainfall event (August 29th). This can be attributed to the fact that when the precipitation reaches its peak, most surface runoff becomes impervious overflow due to the limited interception capacity of BUSNs. However, as the rainfall subsides and surface runoff decreases, the contribution from the BUSN outflow increases due to the delayed release.

Further analyzing the flood reduction effect of BUSNs, we compute the flood reduction percentage as follows:

$$\gamma = \frac{Q_{pwo} - Q_{pw}}{Q_{pwo}} \times 100$$

where γ, Q_{pwo} and Q_{pw} are peak reduction percentage, peak discharge without BUSN during a rainfall event, and peak discharge with BUSN during the same event, respectively. We find that the flood reduction effect increases with the imperviousness and interception capacity of BUSNs, by up to 50%. This effect weakens substantially from August 27 to 28 and then 29, since the transient storage capacity of BUSNs has been reached, so less and less stormwater can be taken by the BUSNs.

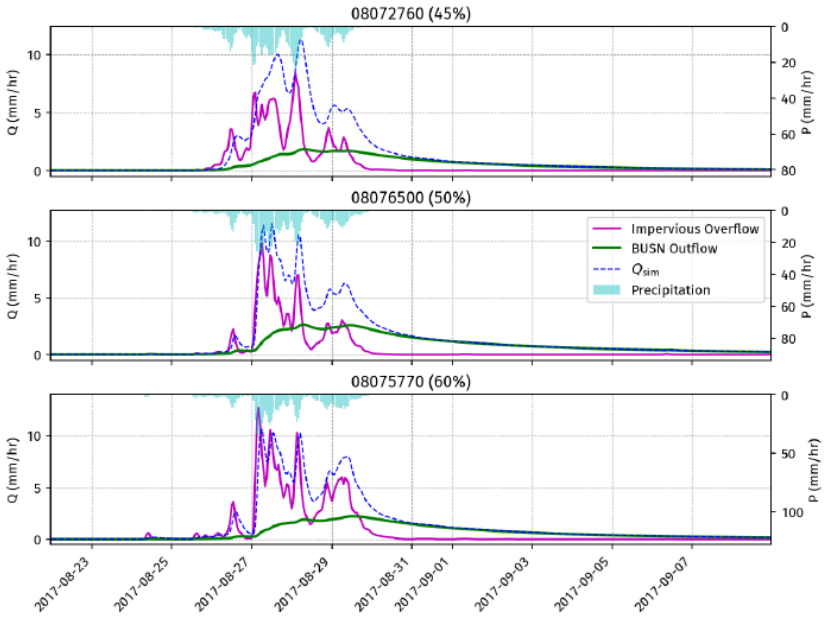

Figure 8. The interplay between hourly rainfall, impervious zone overflow, and BUSN outflow during Hurricane Harvey at three watersheds with high imperviousness. The total streamflow (Q_{sim}) is the sum of the impervious overflow and BUSN overflow.

3.2 Results From ELM Calibration

While Section 3.1 presents an evaluation and analysis of MOSART-urban simulations in the Houston metropolitan areas, the model was configured to simulate both runoff and streamflow as a standalone model. As a first step to integrate MOSART-urban into E3SM, we test the coupling of MOSART-urban with ELM by using the surface and subsurface runoff simulated by ELM as input to MOSART-urban, by-passing the runoff module within MOSART-urban to simulate streamflow. As described in Section 2.2, ELM was calibrated using benchmark WTD and inundated surface water fraction data. Model calibration significantly improved ELM's simulation of WTD and f_{ssw} (**Error! Reference source not found.**). The benchmark dataset shows deeper WTD in the Western, Mid-Atlantic, and Northeastern CONUS (**Error! Reference source not found.**a). While the ELM simulation with the default f_{drain} values lacks spatial variability in simulated WTD (**Error! Reference source not found.**b), the simulation with calibrated f_{drain} can reproduce the WTD spatial variability of the benchmark dataset. On all three statistical metrics (i.e., bias, root mean square error (RMSE), and spatial correlation (R2)), the calibrated model shows significant improvements as compared to the default model. Similarly, f_c calibration improved the prediction of surface water dynamics. The default model predicted much higher f_{ssw} values for the Central and Eastern CONUS (**Error! Reference source not found.**e) than those in the GLAD dataset (**Error!**

Reference source not found.d). After calibration, the overestimation of f_{ssw} was corrected, with a significantly improved R2 from 0.14 to 0.67.

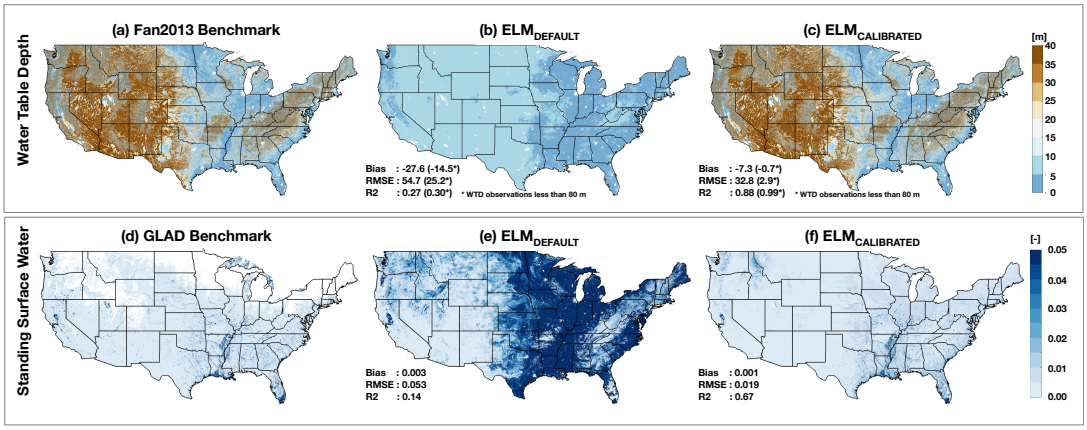

Figure 9. Evaluation of ELM-simulated water table depth (WTD) and standing surface water dynamics. (a) Benchmark WTD dataset of Fan et al. (2013) and ELM-simulated WTD with (b) default f_{drain} and (c) calibrated f_{drain}. (d) Benchmark inundated surface water fraction, f_{ssw}, dataset and ELM-simulated f_{ssw} with (e) default f_c and (f) calibrated f_c.

3.3 CONUS-Wide MOSART-urban Simulations Driven by the ELM Runoff

This section focuses on the evaluation and analysis of MOSART-urban driven by the runoff simulated by the calibrated ELM described in Section 3.2. The evaluation was performed over the 299 urban watersheds shown in Figure 4 with no less than 30% of urban area coverage. Overall, MOSART-urban (with BUSN) performs reasonably well, as shown in Figure 10. The KGE values are above 0.4 (great performance), between 0.0 and 0.4 (satisfactory performance), and below 0.0 (not ideal performance) at 41, 153, and 105 stations, respectively. Satisfactory performance was obtained at about 65% of the urban watersheds.

Figure 10. KGE at the selected USGS stations with significant urban developments in their drainage areas.

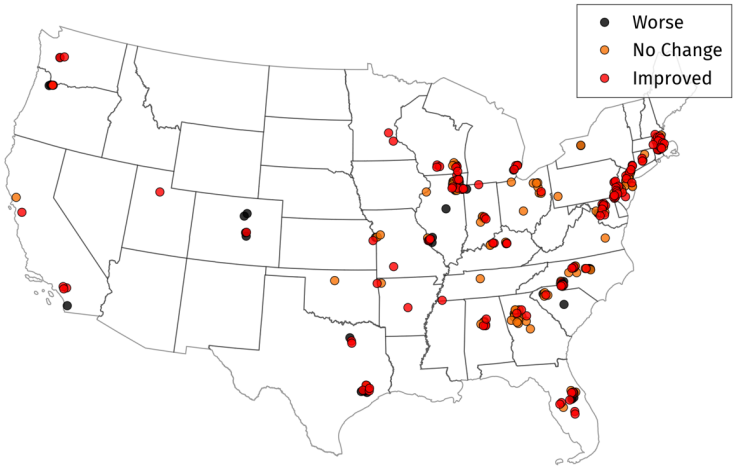

Figure 11. Change of the KGE values between simulations with and without BUSNs.

To understand the net effects of BUSNs in urban hydrology, we examined the changes in KGE values over the 299 USGS stations by comparing the KGE values of the MOSART-urban simulations with and without BUSNs, as shown in Figure 11. Here, "improved", "no change", and "worse" refer to the KGE changes larger than 0.05, within -0.05~0.05, and less than -0.05, respectively. With the BUSN representation, the model performance was improved at 126 stations, compared to 54 stations where the performance was degraded. The cause of worse performance is likely due to several reasons: 1) uncertainties in the NLDAS2 atmospheric forcing driving ELM; 2) theoretical limitations in the current ELM runoff scheme inherited from the Community Land Model (CLM4.5) (Oleson et al. 2013); and 3) the ELM parameter calibration described in Section 2.2 was conducted to target improvements in simulating groundwater table and inundated surface water fraction, not runoff which was used as input to MOSART-urban.

To more comprehensively evaluate MOSART-urban and the impact of including BUSNs, Figure 12 compares the KGE, R^2, and NRMSE between the MOSART-urban simulations with and without BUSNs. Overall, with BUSN, the model performance is better in terms of KGE and NRMSE but not so in terms of R^2, suggesting that adding BUSNs helps to simulate the magnitude of daily streamflow more accurately but has little impact on the timing of streamflow at the daily timescale. The latter has been noted in the analysis of the MOSART-urban simulation during Hurricane Harvey (Section 3.1). Generally, the temporal variations of streamflow in urban watersheds are more dominated by the temporal variability of weather variables such as precipitation, particularly for watersheds with relatively small drainage areas.

To examine the flood-mitigation effects of BUSNs in detail, we selected four representative urban watersheds, with areal urban fractions of 30%, 53%%, 77%, and 98%, respectively. Figure 13 suggests that BUSNs reduce flood peaks of various magnitudes. Importantly, such flood mitigation effects increase with urban fractions in the basins, i.e., more significant effects in the watersheds with more urban areas. Generally, the higher the urban fractions, the denser the BUSNs within a river basin, and the larger the BUSNs' flood-mitigation capacities.

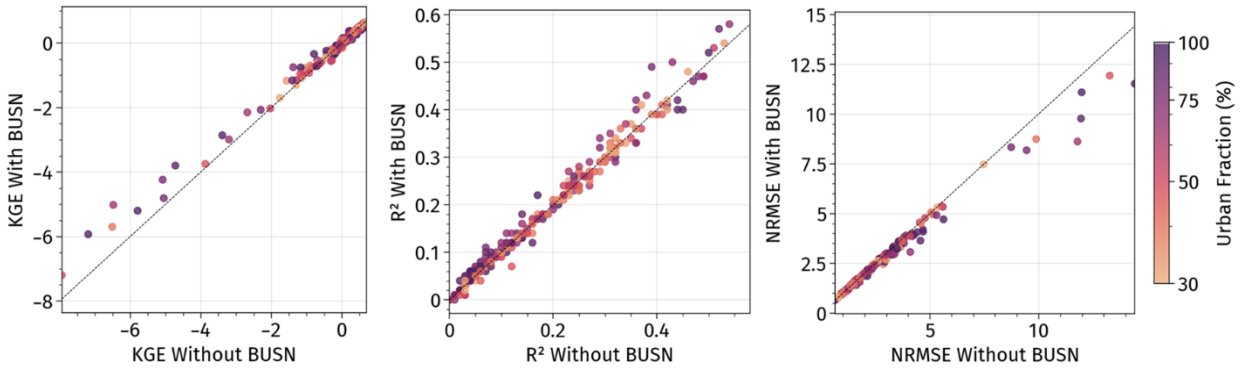

Figure 12. Scatter plots of KGE, R2, and NRMSE between MOSART-urban simulations with and without BUSNs. Higher KGE and lower NRMSE values for the simulation with BUSN than without BUSN indicate improvements in simulating the magnitude of daily streamflow when BUSNs are included in the model.

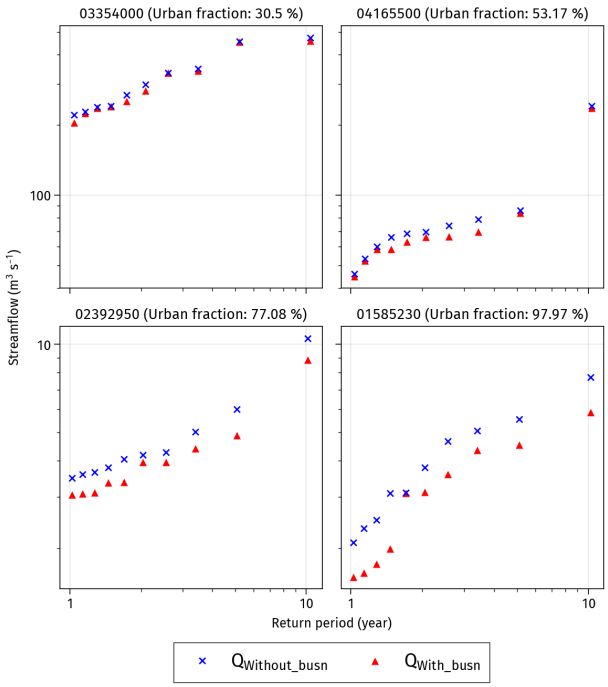

Figure 13. Comparison of annual maximum daily flood peaks, shown as the AMF for different return periods, at four representative stations simulated by MOSART-urban with and without BUSNs. The areal urban fractions of the four stations are shown by the numbers inside the parenthesis above each panel.

4.0 Summary and Future Work

The development of MOSART-urban has filled an important gap between large-scale hydrologic models and hydraulic-based models by introducing and demonstrating a new modeling and parameterization strategy. This new strategy centers on a network-level representation of stormwater pipes that can sufficiently well capture the major hydrologic functions of BUSNs, namely interception, conveyance, and transient storage of urban runoff. This approach allows for an explicit representation of BUSNs in watershed-scale modeling, overcoming a significant limitation in previous large-scale

modeling. Our BUSN parameterization benefits from several Graph-Theory-based algorithms, such as Depth-First Search and community detection. The network-level presentation and parameterization help reduce computational burden in two ways: 1) it avoids computations at individual pipes and their interactions; 2) it avoids hydraulic-based governing equations, which typically invoke more detailed calculations than hydrologic equations.

Validation against observed daily streamflow at USGS stations shows that MOSART-urban can capture small-to-large flood peaks and seasonal and annual water balance over the nine watersheds in the Houston area. Notably, MOSART-urban demonstrates better performance compared to the National Water Model, which is a higher complexity model developed by NOAA for streamflow forecasting. Toward integrating MOSART-urban in E3SM, MOSART-urban simulations driven by the runoff simulated by ELM show good performance in ~65% of the 299 watersheds across CONUS, with an urban fraction > 30%. Comparisons of MOSART-urban with and without BUSNs for both the simulations over the Houston metropolitan area and across CONUS demonstrate the flood-mitigation capacity of BUSNs, which increases with the urban area coverage in the watersheds. MOSART-urban bridges the gap between detailed hydraulic and large-scale hydrologic models, providing a valuable tool for urban flood prediction and management across broader spatial and temporal scales and for Earth system modeling of the impacts of urbanization on the regional and global water cycles.

Future research will address several limitations in MOSART-urban, such as including sanitary sewage and pollutants and additional urban infrastructure, such as stormwater detention/retention ponds. Currently, MOSART-urban only simulates peak flows. Adding inundation dynamics will allow the model to simulate inundation in urban areas for investigation of compound flooding events such as those related to hurricane-induced storm surges and inland river discharge. Noting that the larger biases in the CONUS-wide MOSART-urban simulations compared to the Houston simulations are partly contributed by biases in the ELM-simulated runoff, efforts will be devoted to further improving ELM for coupling with MOSART-urban. While ELM parameters were calibrated to improve the simulation of water table and surface water dynamics, parameters were not calibrated to improve runoff generation in ELM. In the future, we will explore using the previously developed surrogate-assisted Bayesian framework of Xu et al. (2022) to calibrate the ELM-simulated runoff for the 1 km CONUS configuration.

5.0 References

Argue, JR, and D Pezzaniti. 2012. Use of WSUD ‘source control’ practices to manage floodwaters in urbanising landscapes: developed and ultra-developed catchments, https://api.semanticscholar.org/CorpusID:202609239

Bisht, G, WJ Riley, GE Hammond, and DM Lorenzetti. 2018. “Development and evaluation of a variably saturated flow model in the global E3SM Land Model (ELM) version 1.0.” *Geoscientific Model Development* 11: 4085-4102, https://doi.org/10.5194/gmd-11-4085-2018

Brown, S, J Schall, J Morris, C Doherty, S Stein, and J Warner. 2009. Urban Drainage Design Manual: Hydraulic Engineering Circular 22, Third Edition Tech Report No. FHWA-NHI-10-009). Federal National Highway Institute, https://www.fhwa.dot.gov/engineering/hydraulics/pubs/10009/10009.pdf

Burns, MJ, Schubert, JE, Fletcher, TD, and Sanders, BF. 2015. "Testing the impact of at-source stormwater management on urban flooding through a coupling of network and overland flow models." *WIREs Water* 2(4): 291–300, http://doi.org/10.1002/wat2.1078

Chegini, T, and H-Y Li. 2022. "An algorithm for deriving the topology of belowground urban stormwater networks." *Hydrology and Earth System Sciences* 26(16): 4279–4300, doi: 10.5194/hess-26-4279-2022

Chegini, T, H-Y Li, YCE Yang, G Blöschl, and L R Leung. 2025. "A Scale-Adaptive Urban Hydrologic Framework: Incorporating Network-Level Storm Drainage Pipes Representation." *Water Resources Research* 61(3), doi:10.1029/2024WR037268

Chen, M, S Nabih, NS Brauer, S Gao, JJ Gourley, Z Hong, RL Kolar, and Y Hong. 2020. "Can Remote Sensing Technologies Capture the Extreme Precipitation Event and Its Cascading Hydrological Response? A Case Study of Hurricane Harvey Using EF5 Modeling Framework." *Remote Sensing* 12(3): 445, https://doi.org/10.3390/rs12030445

Chocat, B, P Krebs, J Marsalek,W Rauch, and W Schilling. 2001. "Urban drainage redefined: from stormwater removal to integrated management." *Water Science & Technology* 43(5): 61–68, https://doi.org/10.2166/wst.2001.0251

Cosgrove, B, D Gochis, T Flowers, A Dugger, F Ogden, T Graziano, E Clark, R Cabell, N Casiday, Z Cui, K Eicher, G Fall, X Feng, K Fitzgerald, N Frazier, C George, R Gibbs, L Hernandez, D Johnson, R Jones, L Karsten, H Kefelegn, D Kitzmiller, H Lee, Y Liu, H Mashriqui, D Mattern, A McCluskey, JL McCreight, R McDaniel, A Midekisa, A Newman, L Pan, C Pham, A RefieeinNasab, R Rasmussen, L Read, M Rezaeianzadeh, F Salas, D Sang, K Sampson, T Schneider, Q Shi, G Sood, A Wood, W Wu, D Yates, W Yu, and Y Zhang. 2024. "NOAA's national water model: Advancing operational hydrology through continental-scale modeling." *JAWRA Journal of the American Water Resources Association* 60(2): 247-272, https://doi.org/10.1111/1752-1688.13184

Durran, DR. 2010. Ordinary Differential Equations. In DR Durran (Ed.), *Numerical Methods for Fluid Dynamics: With Applications to Geophysics* (pp. 35–87). New York, NY: Springer. http://doi.org/10.1007/978-1-4419-6412-0_2

Fan, Y, H Li, and G Miguez-Macho. 2013. "Global patterns of groundwater table depth." *Science* 339: 940-943, https://doi.org/10.1126/science.1229881

Golaz, J-C, LP Van Roekel, X Zheng, AF Roberts, JD Wolfe, W Lin, W, AM Bradley, Q Tang, ME Maltrud, RM Forsyth, C Zhang, T Zhou, K Zhang, CS Zender, M Wu, H Wang, AK Turner, B Singh, JH Richter, Y Qin, MR Petersen, A Mametjanov, P-L Ma, VE Larson, J Krishna, ND Keen, N Jeffery, EC Hunke, WM Hannah, O Guba, BM Griffin, Y Feng, D Engwirda, AV Di Vittorio, C Dang, LM Conlon, C-C-J Chen, MA Brunke, G Bisht, JJ Benedict, XS Asay-Davis, Y Zhang, M Zhang, X Zeng, S Xie, PJ Wolfram, T Vo, M Veneziani, TK Tesfa, S Sreepathi, AG Salinger, JEJ Reeves Eyre, MJ Prather, S Mahajan, Q Li, PW Jones, RL Jacob, GW Huebler, X Huang, BR Hillman, BE Harrop, JG Foucar, Y Fang, DS Comeau, PM Caldwell, T Bartoletti, K Balaguru, MA Taylor, RB McCoy, LR Leung, and DC Bader. 2022. "The DOE E3SM Model version 2: Overview of the physical model and initial model evaluation." *Journal of Advances in Modeling Earth Systems* 14(12), https://doi.org/10.1029/2022MS003156

Grimm, NB, SH Faeth, NE Golubiewski, CL Redman, J Wu, X Bai, and JM Briggs. 2008. "Global change and the ecology of cities." *Science* 319(5864):756–760, https://doi.org/10.1126/science.1150195

Guo, K, M Guan, and D Yu. 2021. "Urban surface water flood modelling – a comprehensive review of current models and future challenges." *Hydrology and Earth System Sciences* 25(5): 2843–2860, https://doi.org/10.5194/hess-25-2843-2021

Hao, D, G Bisht, Y Gu, W-L Lee, K-N Liou, and LR Leung. 2021. "A parameterization of sub-grid topographic effects on solar radiation in the E3SM Land Model (version 1.0): Implementation and evaluation over the Tibetan Plateau." *Geoscientific Model Development* 14: 6273-6289, https://doi.org/10.5194/gmd-14-6273-2021

Li, H, MS Wigmosta, H Wu, M Huang, Y Ke, AM Coleman, and LR Leung, 2013. "A Physically Based Runoff Routing Model for Land Surface and Earth System Models." *Journal of Hydrometeorology* 14 (3): 808–828, doi:10.1175/JHM-D-12-015.1

Li, L, G Bisht, D Hao, and LR Leung. 2024. "Global 1 km land surface parameters for kilometer-scale Earth system modeling." *Earth System Science Data* 16(4): 2007–2032, https://doi.org/10.5194/essd-16-2007-2024

Miller, JD and Hutchins, M. 2017. "The impacts of urbanisation and climate change on urban flooding and urban water quality: A review of the evidence concerning the united kingdom." *Journal of Hydrology: Regional Studies* 12: 345–362, https://doi.org/10.1016/j.ejrh.2017.06.006

Oleson, KE, DM Lawrence, GB Bonan, A Bozbiyik, B Drewniak, M Huang, E Kluzek, CD Koven, J-F Lamarque, PJ Lawrence, LR Leung, S Levis, F Li, WJ Riley, W Sacks, ZM Subin, SC Swenson, PE Thornton. 2013. "Technical Description of Version 4.5 of the Community Land Model (CLM)." NCAR Technical Note, NCAR/TN-503+STR, National Center for Atmospheric Research, Boulder, CO, 434 pp. https://doi.org/10.5065/D6RR1W7M

Pickens, AH, MC Hansen, M Hancher, SV Stehman, A Tyukavina, P Potapov, B Marroquin, and Z Sherani. 2020. "Mapping and sampling to characterize global inland water dynamics from 1999 to 2018 with full Landsat time-series." *Remote Sensing of Environment* 243, https://doi.org/10.1016/j.rse.2020.111792

Xia, Y, K Mitchell, M Ek, J Sheffield, B Cosgrove, E Wood, L Luo, C Alonge, H Wei, J Meng, B Livneh, D Lettenmaier, V Koren, Q Duan, K Mo, Y Fan, and D Mocko. 2012. "Continental-scale water and energy flux analysis and validation for the North American Land Data Assimilation System project phase 2 (NLDAS-2):1. Intercomparison and application of model products." *Journal of Geophysical Research: Atmospheres* 117(D3), https://doi.org/10.1029/2011JD016048

Xu, D, G Bisht, Z Tan, E Sinha, P Megonigal, AV Di Vittorio, T Zhou, VY Ivanov, and LR Leung. 2024. "Climate change will reduce North American inland wetland areas and disrupt their seasonal regimes." *Nature Communications* 15: 2438, https://doi.org/10.1038/s41467-024-45286-z

Xu, D, G Bisht, K Sargsyan, C Liao, and LR Leung. 2022. "Using a Surrogate-Assisted Bayesian Framework to Calibrate the Runoff Generation Scheme in Energy Exascale Earth System Model (E3SM) v1." *Geoscientific Model Development* 15: 5021-5043, https://doi.org/10.5194/gmd-15-5021-2022

Yang, L, JA Smith, DB Wright, ML Baeck, G Villarini, F Tian, and H Hu. 2013. "Urbanization and climate change: An examination of nonstationarities in urban flooding." *Journal of Hydrometeorology* 14(6): 1791–1809, https://doi.org/10.1175/JHM-D-12-095.1

U.S. DEPARTMENT OF
ENERGY

Office of Science